

The effect of paramagnetic impurities in normal metal on the critical current in a network of S–N–S Josephson junctions in bulk $Y_{3/4}Lu_{1/4}Ba_2Cu_3O_7 + BaPb_{1-x}Fe_xO_3$ composites

To cite this article: D A Balaev *et al* 2002 *Supercond. Sci. Technol.* **16** 60

View the [article online](#) for updates and enhancements.

Related content

- [Magneto-resistive effect in bulk composites 1-2-3 YBCO + CuO and 1-2-3 YBCO + BaPb_xSn_{1-x}O₃ and their application as magnetic field sensors at 77 K](#)
D A Balaev, K A Shalhutdinov, S I Popkov *et al.*
- [Correlation of the electric field effect with the weak link behaviour in granular YBCO superconductors](#)
T S Orlova, B I Smirnov, J Y Laval *et al.*
- [Study of dependence upon the magnetic field and transport current of the magneto-resistive effect in YBCO-based bulk composites](#)
D A Balaev, A G Prus, K A Shaykhtudinov *et al.*

Recent citations

- [Crossover from the “clean” limit to the “dirty” limit in a network of S-N-S weak links in \$Y_{3/4}Lu_{1/4}Ba_2Cu_3O_7 + BaPb_{1-x}Sn_xO_3\$ \(0 ≤ x ≤ 0.25\) composites](#)
M. I. Petrov *et al*



IOP | ebooks™

Bringing together innovative digital publishing with leading authors from the global scientific community.

Start exploring the collection—download the first chapter of every title for free.

The effect of paramagnetic impurities in normal metal on the critical current in a network of S–N–S Josephson junctions in bulk $Y_{3/4}Lu_{1/4}Ba_2Cu_3O_7 + BaPb_{1-x}Fe_xO_3$ composites

D A Balaev, S V Ospishchev, M I Petrov and K S Aleksandrov

Kirensky Institute of Physics, 660036 Krasnoyarsk, Russia

E-mail: smp@iph.krasn.ru

Received 14 June 2002

Published 10 December 2002

Online at stacks.iop.org/SUST/16/60

Abstract

Bulk $Y_{3/4}Lu_{1/4}Ba_2Cu_3O_7 + BaPb_{1-x}Fe_xO_3$ composites representing a model of a network of superconductor–normal metal–superconductor (SNS) Josephson junctions with paramagnetic impurities (Fe) in the N layers have been prepared. The transport properties of the composites have been studied. An exponential decay of the critical current with increasing Fe content in the non-superconducting ingredient of the composite has been observed. Such a behaviour is accounted for in terms of the de Gennes proximity effect theory.

1. Introduction

Investigations of SNS (where S is a superconductor, and N is a normal metal) Josephson junctions with magnetic impurities in the N layer are of considerable theoretical [1–7] and experimental [8–15] interest. This is due to the possibility of studying such interesting phenomena as π -coupling [1–3, 6, 7, 15, 16], and suppression of critical current by spin-flip scattering [5, 8, 9, 12, 13]. Two different impurity concentration (n) ranges can be distinguished: $n \ll 1$ (non-interacting spins) and $n \leq 1$, in which magnetic interaction may lead to magnetic ordering in the N layer. The latter case was studied in [15, 16], with oscillations of critical current observed and possible practical application pointed out [16]. The effect of magnetic impurities in the N layer at small impurity concentrations ($n \ll 1$, which is the subject of the present paper) on the critical current j_c has been studied experimentally for SNS Josephson junctions based on conventional superconductors [8, 9]. CuMn and AgMn alloys have been used as materials for N layers [8, 9]. A similar study of Josephson junctions based on high temperature superconductors (HTSC) would be rather interesting, since it could contribute to the understanding of the nature of high temperature superconductivity [17, 18].

Metal-oxides seem to be good candidates for use as materials for N layers between HTSC ‘banks’ [11–13]. YBCO/Co-doped YBCO/YBCO junctions were studied in [12, 13] and the $j_c(T)$ data obtained were processed using the conventional de Gennes proximity effect theory [19]. A study of this kind encounters serious technological problems associated with introducing a controlled amount of impurity atoms into the N layer of very small thickness and obtaining an edge S–N interface, because of the high chemical activity of HTSC [17, 20]. On the other hand, HTSC-based composites are a typical example of a weak-link network with a non-superconducting component playing the role of barriers separating the HTSC crystallites [21–31]. Although the transport properties of such composites are affected by the distribution function of the geometrical parameters of the non-superconducting layers [32], nevertheless, the main features of the resistive state of the composites remain the same as those of some single weak links [24, 26, 28, 31]. For example, the HTSC + insulator composites prepared by us [28] demonstrate current–voltage (I – V) characteristics having excess voltage, and a broad resistive transition is successfully described by the mechanism of thermally activated phase slippage [33], developed for SIS (where I is insulator) structures.

The composites HTSC + $BaPbO_3$ have been shown to be a model of a network of weak SNS links in the ‘clean’

limit [24, 26] (the mean free path $l \sim 220 \text{ \AA}$ [34] is larger than the coherence length ξ_0 , $l > \xi_0$). I – V characteristics of composites with normal metal possess excess current and hysteretic peculiarity [26]. The latter feature reflects the part with negative differential resistance [35]. The temperature dependences of the critical current in HTSC + BaPbO₃ composites [24] have been successfully described within the framework of a theory [36] developed for ‘clean’ SNS junctions. Although the ceramic technique allows one to introduce a controlled amount of impurities into a metal oxide by the simplest way, it is advisable to investigate the effect of magnetic scattering centres in BaPbO₃ on the transport properties of HTSC + BaPbO₃ composites. In [29], the effect of various impurities in BaPb_{0.9}Met_{0.1}O₃ (Met = Sn, Ni, Fe) on the transport properties of HTSC + BaPb_{0.9}Met_{0.1}O₃ composites was studied. The pair-breaking effect associated with the interaction between supercurrent carriers and the magnetic moments of impurity atoms has been observed [29]. In the present study, we compare the critical current density of HTSC + BaPb_{1-x}Fe_xO₃ composites (x is the concentration of Fe atoms), with the $j_c(x, T)$ data obtained on composites with fixed volume content of non-superconducting ingredient. So the distribution function of the N layers is assumed to be the same for all the samples. For this reason, the changes in $j_c(x, T)$ dependence of the composites can be attributed to the modification of pair propagation through layers formed by the non-superconducting component.

2. Experimental details

2.1. Synthesis and magnetic properties of BaPb_{1-x}Fe_xO₃ compounds

The non-superconducting ingredients BaPb_{1-x}Fe_xO₃ ($x = 0, 0.0375, 0.1$) were synthesized from the oxides BaO₂, PbO, Fe₂⁵⁷O₃ at 880 °C by the solid state reaction technique. The use of hematite enriched in Fe⁵⁷ isotope to 90% allowed us to monitor the iron ‘solubility’ in the BaPbO₃ structure during synthesis by means of the Mossbauer technique. It has been established that, after two weeks of sintering with daily grinding, the six-line Mossbauer spectrum of hematite disappeared. The synthesis was prolonged additionally for a week. X-ray diffraction patterns of the compounds obtained show the same reflections of the perovskite structure as pure BaPbO₃, without any additional reflections or changes in the lattice constant.

Magnetic measurements have been performed on samples with $x = 0.0375$ and 0.1 . Figure 1 shows magnetization curves $M(H)$ for these samples at 4.2 K. By juxtaposition of the experimental $M(H)$ curves with the Brillouin function, the magnetic moment per Fe atom was found to be $\sim 3.6 \mu_B$ (where μ_B is the Bohr magneton). This value is intermediate between that for bulk iron ($2.23 \mu_B$) and the Fe⁴⁺ ion (4.9 – $5.4 \mu_B$) [37]. The total spin of Fe²⁺ is equal to that for Fe⁴⁺ ions occupying octahedral positions, because these ions have identical electron configurations [37]. This means that pairwise interaction of Fe atoms may take place and result in a reduced magnetic moment per Fe atom. On the other hand, the absence of hysteresis in the $M(H)$ curves and the $1/T$ dependence of magnetization measured at $H = 3 \text{ kOe}$ in

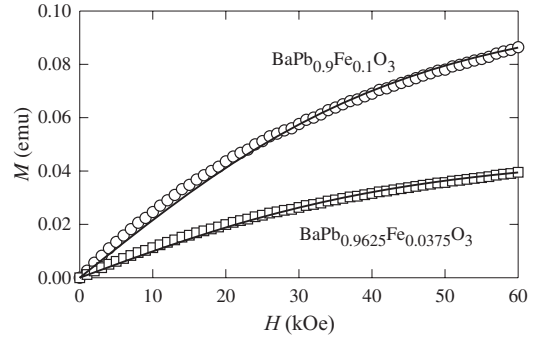


Figure 1. Magnetization versus field $M(H)$ dependences for BaPb_{0.9625}Fe_{0.0375}O₃ ($m = 96 \text{ mg}$), and BaPb_{0.9}Fe_{0.1}O₃ ($m = 112 \text{ mg}$) compounds (symbols). Full curves are fits with Brillouin function for $J = 1$.

the temperature range 4.2–100 K (not shown) indicate that the compounds obtained are paramagnetic.

The resistivity ρ of BaPb_{1-x}Fe_xO₃ at 4.2 K is $\sim 0.55 \text{ m}\Omega \text{ cm}$ for $x = 0$, $\sim 0.02 \text{ }\Omega \text{ cm}$ for $x = 0.0375$ and $\sim 3 \text{ }\Omega \text{ cm}$ for $x = 0.1$. The rise in ρ with increasing x is much higher than that for the case of Sn substitution for Pb in BaPbO₃ (for BaPb_{0.9}Sn_{0.1}O₃ $\rho(4.2 \text{ K}) \approx 0.02 \text{ }\Omega \text{ cm}$) [26]. This behaviour is in agreement with the interaction mechanism of charge carriers with non-magnetic and magnetic impurities [38].

2.2. Preparation and characterization of

$Y_{3/4}Lu_{1/4}Ba_2Cu_3O_7 + BaPb_{1-x}Fe_xO_3$ composites

$Y_{3/4}Lu_{1/4}Ba_2Cu_3O_7$ HTSC was prepared by the standard procedure. Composite samples with different volume contents of HTSC and BaPb_{1-x}Fe_xO₃ ($x = 0, 0.0375, 0.1$) were prepared as follows. The components of the composite were thoroughly mixed, with additional joint milling of the powders in an agate mortar, and then pressed into pellets. The pellets were placed in preheated boats and then introduced into a furnace heated to 930 °C. The pellets were kept at this temperature for 5 min and then placed in another furnace for 6 h at 400 °C, which was followed by furnace-cooling to room temperature. In order to recognize the effect of increasing Fe content of BaPb_{1-x}Fe_xO₃ on the transport properties of the composites and to exclude the influence of accidental technological factors, a set of samples with a constant volume content of BaPb_{1-x}Fe_xO₃ was prepared simultaneously. Three sets of composites with 7.5, 15 and 22.5 vol% BaPb_{1-x}Fe_xO₃ were prepared and studied. A qualitatively similar behaviour with increasing x has been observed for all the sets. This paper presents the results obtained for composite samples with 85 vol% $Y_{3/4}Lu_{1/4}Ba_2Cu_3O_7$ and 15 vol% BaPb_{1-x}Fe_xO₃. Hereafter we denote samples by the Fe content of BaPb_{1-x}Fe_xO₃: S + Fe0, S + Fe0375 and S + Fe10 (e.g., sample S + Fe0375 is a composite containing 85 vol% $Y_{3/4}Lu_{1/4}Ba_2Cu_3O_7$ and 15 vol% BaPb_{0.9625}Fe_{0.0375}O₃).

X-ray diffraction patterns of the composites confirmed the presence of both the 1–2–3 and the perovskite structures without any additional reflections. The average YBCO grain size was estimated from an SEM micrograph to be $1.5 \text{ }\mu\text{m}$. The temperature dependences of magnetization $M(T)$ of the composites, measured in an external field

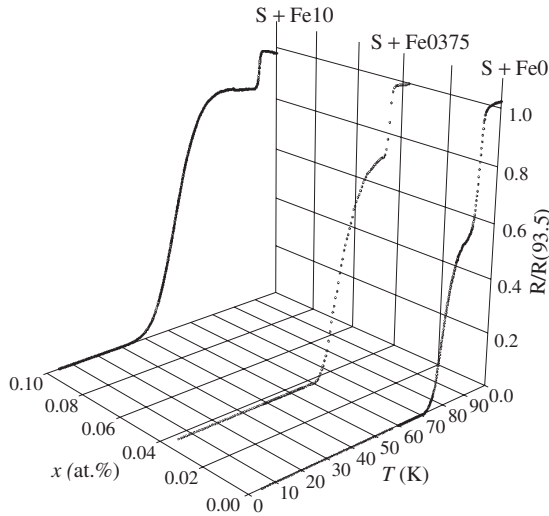


Figure 2. Temperature dependences of normalized resistivity $R(T)/R(93.5 \text{ K})$ for the composites as a function of Fe content in $\text{BaPb}_{1-x}\text{Fe}_x\text{O}_3$.

of 300 Oe in the temperature range 4.2–100 K, revealed a single superconducting phase in the samples, with a critical temperature $T_c = 93.5 \text{ K}$ similar to that in pure $\text{Y}_{3/4}\text{Lu}_{1/4}\text{Ba}_2\text{Cu}_3\text{O}_7$. No essential difference between the $M(T)$ curves was observed for composite samples with different Fe doping levels in $\text{BaPb}_{1-x}\text{Fe}_x\text{O}_3$.

2.3. Electrical measurements

To measure the resistivity R and the critical current, a sample was cut from a sintered pellet in the form of parallelepiped with typical dimensions $2 \times 2 \times 10 \text{ mm}^3$. The standard four-probe technique was used. The critical current was determined from the initial part of the $I-V$ characteristics, using the standard $1 \mu\text{V cm}^{-1}$ criterion [39]. Variation of the critical current density j_c from sample to sample of a pellet was less than 3%. The $R(T)$ dependences presented below were measured with transport dc current $j \approx 0.01 j_c(5\text{K})$. Lowering the current j affects the $R(T)$ curves only slightly (by less than 2%), but raising j has a strong effect on these curves, especially as regards the ‘zero resistivity’ T_c ($\rho < 10^{-6} \Omega \text{ cm}$).

3. Results and discussion

Figure 2 shows normalized resistivity versus temperature curves for composites with different Fe contents in $\text{BaPb}_{1-x}\text{Fe}_x\text{O}_3$. A sharp drop of resistance at 93.5 K, appearing at any probing current is caused by the transition in HTSC crystallites. The critical temperature $T_c = 93.5 \text{ K}$ coincides with that determined by magnetic measurements (see section 2.2). A broad-foot structure results from a transition in the network of weak links. The zero resistivity temperature decreases with increasing Fe content in $\text{BaPb}_{1-x}\text{Fe}_x\text{O}_3$. Previously, a decrease in this temperature, $T_c(R = 0)$, has been observed for HTSC + Normal-metal composites with increasing metal content, i.e. with growing effective N layer thickness in the composites [24, 25]. For the composites under study this effect is attributed to suppression of superconducting properties by interaction

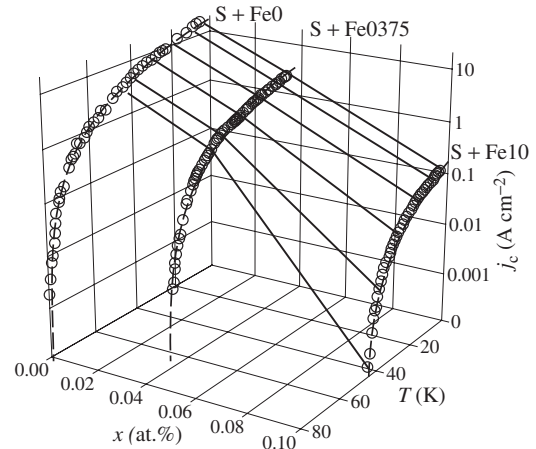


Figure 3. Critical current density (logarithmic scale) $j_c(T, x)$ for the composites versus temperature and Fe content in $\text{BaPb}_{1-x}\text{Fe}_x\text{O}_3$. Broken curves are the best fits with equation (1) obtained at $j_c(0 \text{ K}) = 18 \text{ A cm}^{-2}$, $T_{cl} = 79.5 \text{ K}$ for S + Fe0, $j_c(0 \text{ K}) = 3.8 \text{ A cm}^{-2}$, $T_{cl} = 66.5 \text{ K}$ for S + Fe0375, $j_c(0 \text{ K}) = 0.185 \text{ A cm}^{-2}$, $T_{cl} = 46 \text{ K}$ for S + Fe10. Solid lines are isotherms $j_c(x)$ at 5 K, 10 K, 20 K, 30 K, 40 K, 45 K.

of carrier spins with the magnetic moments of Fe atoms in the N layers. With increasing Fe content, there is a tendency for the $R(T)$ region below T_c to become weakly temperature dependent. Similar kinks have been observed in the $R(T)$ curves of composites $\text{YBCO} + \text{Cu}_{1-x}\text{Ni}_x\text{O}$ [40] and $\text{YBCO} + \text{NiTiO}_3$ [30] and single Josephson junctions with ferromagnetic barriers $\text{YBa}_2\text{Cu}_3\text{O}_7/\text{Pr}_{0.7}\text{Sr}_{0.3}\text{MnO}_3/\text{Ag}$, $\text{YBa}_2\text{Cu}_3\text{O}_7/\text{Pr}_{0.7}\text{Sr}_{0.3}\text{MnO}_3/\text{YBa}_2\text{Cu}_3\text{O}_7$ [11] and $\text{Nb}/\text{Al}/\text{Gd}/\text{Al}/\text{Gd}/\text{Nb}$ [14]. Regardless of the barrier type (metal, insulator), the presence of magneto-active atoms in the barrier between the superconductors results in a specific shape of $R(T)$ below the transition temperature of the ‘superconductors’.

Figure 3 shows experimental $j_c(T)$ dependences of the composites. The X, Y and Z axes correspond to, respectively, the Fe content, temperature and critical current density (logarithmic scale). We first consider the temperature dependences of j_c . The shape of $j_c(T)$ does not change dramatically with increasing Fe content in $\text{BaPb}_{1-x}\text{Fe}_x\text{O}_3$. All $j_c(T)$ data are found to follow the quadratic law:

$$j_c(T) \sim j_c(0 \text{ K}) \left(1 - \frac{T}{T_{cl}}\right)^2, \quad (1)$$

where $j_c(0 \text{ K})$ is the critical current density at 0 K, and T_{cl} is the temperature at which j_c values become vanishingly small (less than $10^{-4} \text{ A cm}^{-2}$). The T_{cl} values decrease with increasing Fe content, in correlation with the $R(T)$ data (figure 2). Broken curves in figure 3 are the best fits to the experimental $j_c(T)$, obtained with equation (1). A quadratic temperature dependence of j_c near T_c has been frequently observed experimentally in both conventional and HTSC-based S–N–S junctions [12, 13, 39, 41] and predicted by the de Gennes proximity effect theory [19] and other theories [2, 3, 5].

Now we analyse the Fe content dependence of the critical current density $j_c(x)$. The full curves in figure 3 are plotted as isotherms. In the low-temperature region (5–20 K), the $j_c(x)$ dependence is seen to follow the exponential law

$j_c \sim \exp(-x)$. The experimental $j_c(T)$ dependences for S–N–S junctions with magnetic impurities in the N layer were described using an approach [8, 9, 12, 13] based on the de Gennes proximity effect theory [19]. According to [9, 12, 13, 39],

$$j_c(T) = C \left(1 - \frac{T}{T_c}\right)^2 \frac{d/\xi_N}{\sinh(d/\xi_N)}, \quad (2)$$

where C is a constant depending on materials forming a weak link, determined in [8, 12, 19]; d is the thickness of the N layer; and ξ_N is the penetration depth of the pairs into the N layer. For a ‘dirty’ N layer, ξ_N is given by the expression [8, 12]

$$\xi_N = \left(\frac{V_F l}{6}\right)^{1/2} \left(\frac{\pi k_B T}{\hbar} + \frac{1}{\tau}\right)^{-1/2}, \quad (3)$$

where V_F is the Fermi velocity, k_B is Boltzmann’s constant, \hbar is Planck’s constant divided by 2π , and τ is the spin-flip scattering time given by [38]

$$\frac{1}{\tau} = \frac{n}{\hbar} \left[\frac{7}{24} \pi N(0) J^2 (S+1) S \right]. \quad (4)$$

Here $N(0)$ denotes the density of states for one spin direction, J is the exchange integral, and S is the spin of the impurity. Assuming that the expression in the square brackets in equation (4) is the same for non-superconducting ingredients of samples under study, and τ is proportional to the ratio of the mean free path to the carrier velocity [38], we find that the coherence length is nearly inversely proportional to the impurity content. For large N-layer thicknesses, $d \gg \xi_N$, the de Gennes expression (2) transforms to $j_c \sim \exp(-d/\xi_N)$ [39], and, taking into account the above speculations, we obtain for a constant thickness of the N layer and a fixed temperature:

$$j_c \sim \exp(-n). \quad (5)$$

This dependence, derived from the conventional de Gennes proximity effect theory, is in qualitative agreement with our experimental data. The condition $d \gg \xi_N$ seems to take place for the composites under study. According to [24], the effective thickness of N layers in the YBCO + 15 vol% BaPbO₃ composite is approximately 100 Å, while our estimation of ξ_N for BaPb_{0.9625}Fe_{0.0375}O₃ even at $\tau = \infty$ is about 10 Å at 5 K. Quantitative processing of the experimental $j_c(x)$ dependences with the use of equations (4) and (2) is problematic because the estimations of V_F are rough and the parameters $N(0)$ and J in equation (4) are unknown.

Among experimental papers cited in section 1, only one [8] studied the critical current densities in SNS junctions for a wide range of impurity contents and N-layer thicknesses. The authors of [8] measured the critical currents of Pb/Cu(Mn)/Pb and Pb/Ag(Mn)/Pb junctions at 4.2 K, with primary attention given to the coherence lengths in the N layers. For this reason, there are no experimental plots of j_c against the impurity concentration n in [8]. In order to derive the j_c versus n dependence, we replotted data from [8] for j_c versus $2d$ at varied n to j_c versus n at constant d . The exponential decay of j_c with impurity content (within the experimental error) takes place at $2d = 400$ nm for Pb/Cu(Mn)/Pb junctions and at $2d = 200$ nm for Pb/Ag(Mn)/Pb junctions.

4. Conclusion

The critical currents in bulk Y_{3/4}Lu_{1/4}Ba₂Cu₃O₇ + BaPb_{1-x}Fe_xO₃ ($0 < x < 0.1$) composites, modelling a network of S–N–S Josephson junctions with paramagnetic impurities in the N layers, have been studied. An exponential decay of j_c with increasing Fe content was observed in the low temperature range. This behaviour, previously reported for Josephson junctions based on conventional superconductors, was accounted for qualitatively in terms of the de Gennes proximity effect theory.

Acknowledgments

The authors thank A D Balaev for his help in magnetic measurements and useful discussions, O A Bayukov for Mossbauer studies, A D Vasilyev for x-ray diffraction patterns, D M Gokhfeld and K A Shaihtudinov for fruitful discussions and technical assistance. The work was supported in part by the 6th Expert Competition of Young Scientists Projects of the Russian Academy of Sciences, grant N55, and by the Russian Foundation for Basic Research program ‘Enisey’ (grant 02-02-97711).

References

- [1] Bulaevskii L N, Kuzii V V and Sobyenin A A 1977 *JETP Lett.* **25** 290
- [2] Buzdin A I, Bulaevskii L N and Panyukov S V 1982 *JETP Lett.* **35** 178
- [3] Bulaevskii L N, Buzdin A I and Panyukov S V 1982 *Solid State Commun.* **44** 539
- [4] Makeev A I, Mitsai Yu N and Shahova N V 1980 *Sov. J. Low Temp.* **5** 650
- [5] Kuplevahskiy S V and Falko I I 1986 *Fiz. Met. Metalloved.* **62** 13
- [6] Buzdin A I, Bujicic B and Kupriyanov M Yu 1992 *Sov. Phys.-JETP* **101** 124
- [7] Fogelström M 2000 *Phys. Rev. B* **62** 11812
- [8] Niemeyer J and von Minnigerode G 1979 *Z. Phys. B* **36** 57
- [9] Paterson J L 1979 *J. Low Temp. Phys.* **35** 371
- [10] Claeson T 1980 *Thin Solid Films* **66** 151
- [11] Xiong G C, Lian G J, Kang J F, Hu Y F, Zhang Y and Gan Z Z 1997 *Physica C* **282–287** 693
- [12] Antogonazza L, Berkowitz S J, Geballe T H and Char K 1995 *Phys. Rev. B* **51** 8560
- [13] Char K 1997 *Physica C* **282–287** 419
- [14] Bourgeois O, Gandit P, Sulpice A, Chaussy J, Lesueur J and Grison X 2001 *Phys. Rev. B* **63** 064517
- [15] Ryazanov V V, Oboznov V A, Rusanov A Yu, Veretennikov A V, Golubov A A and Aarts A A 2001 *Phys. Rev. Lett.* **86** 2427
- [16] Ryazanov V V, Oboznov V A, Veretennikov A V, Rusanov A Yu, Golubov A A and Aarts A A 2001 *Proc. Int. Conf. Microscopic and Strongly Correlated Systems 2000 (Chernogolovka) Suppl. Usp. Fiz. Nauk* **171** 81
- [17] Borukhovich A S 1999 *Usp. Fiz. Nauk* **169** 737
- [18] Tanaka Y and Kashiwaya S 2000 *J. Phys. Soc. Japan* **69** 1152
- [19] De Gennes P G 1964 *Rev. Mod. Phys.* **36** 225
- [20] Kupriyanov M Yu and Likharev K K 1991 *Usp. Fiz. Nauk* **160** 49
- [21] Calabrese J J, Dubson M A and Garland J C 1992 *J. Appl. Phys.* **72** 2958
- [22] Jung J, Mohamed M A-K, Isaak I and Friedrich L 1994 *Phys. Rev. B* **49** 12188

-
- [23] Tarenkov V Yu, D'yachenko A I and Vasilenko A V 1994 *Phys. Solid State* **36** 1197
- [24] Petrov M I, Balaev D A, Ospishchev S V, Shaihtudinov K A, Khrustalev B P and Aleksandrov K S 1997 *Phys. Lett. A* **237** 85
- [25] Petrov M I, Balaev D A, Ospishchev S V, Shaihtudinov K A, Khrustalev B P and Aleksandrov K S 1997 *Phys. Solid State* **39** 362
- [26] Petrov M I, Balaev D A, Gohfeld D M, Ospishchev S V, Shaihtudinov K A and Aleksandrov K S 1999 *Physica C* **314** 51
- [27] Berling D, Loegel B, Mehdaoui A, Regnier S, Caranoni C and Marfaing J 1998 *Semicond. Sci. Technol.* **11** 1292
- [28] Petrov M I, Balaev D A, Shaihtudinov K A and Aleksandrov K S 1999 *Phys. Solid State* **41** 881
- [29] Petrov M I, Balaev D A, Ospishchev S V, Khrustalev B P and Aleksandrov K S 1997 *Physica C* **282–287** 2447
- [30] Petrov M I, Balaev D A and Shaihtudinov K A 2001 *Physica C* **361** 45
- [31] Petrov M I, Balaev D A, Shaihtudinov K A and Aleksandrov K S 2001 *Supercond. Sci. Technol.* **14** 798
- [32] Meilikhov E Z 1993 *Usp. Fiz. Nauk* **163** N3 27
- [33] Ambegaokar V and Halperin B I 1969 *Phys. Rev. Lett.* **22** 1364
- [34] Kitazawa K, Katsui A, Toriumi A and Tanaka S 1984 *Solid State Commun.* **52** 459
- [35] Kümmel R, Gunsenheimer U and Nicolsky R 1990 *Phys. Rev. B* **42** 3992
- [36] Gunsenheimer U, Schüssler U and Kümmel R 1994 *Phys. Rev. B* **49** 6111
- [37] Krupička S 1973 *Physik der Ferrite* vol 1 (Praga)
- [38] Abrikosov A A 1987 *Osnovy Teorii Metallov (Foundations of Theory of Metals)* (Moscow: Nauka)
- [39] Barone A and Paterno J 1982 *Physics and Application of the Josephson Effect* (New York: Wiley)
- [40] Petrov M I, Balaev D A, Shaihtudinov K A and Ovchinnikov S G 1998 *Phys. Solid State* **40** 1451
- [41] Likharev K K 1979 *Rev. Mod. Phys.* **51** 101